

On solar protons and polar cap absorption: constraints on an empirical relationship

A. J. Kavanagh^{1,2}, S. R. Marple³, F. Honary³, I. W. McCrea⁴, and A. Senior³

¹High Altitude Observatory (HAO), National Center for Atmospheric Research (NCAR), PO Box 3000, Boulder, Colorado, 80307-3000, USA

²Formerly of the Department of Communication Systems, Lancaster University, Lancaster, UK and the EISCAT Group, Space Science and Technology Department, Rutherford Appleton Laboratory, Chilton, Didcot, Oxfordshire, UK

³Department of Communication Systems, Lancaster University, Lancaster, UK

⁴EISCAT Group, Space Science and Technology Dept., Rutherford Appleton Laboratory, Chilton, Didcot, Oxfordshire, UK

Received: 16 June 2003 – Revised: 4 September 2003 – Accepted: 21 October 2003 – Published: 2 April 2004

Abstract. A large database of Solar Proton Events (SPE) from the period 1995 to 2001 is used to investigate the relationship between proton flux at geostationary orbit and Cosmic Noise Absorption (CNA) in the auroral zone. The effect of solar illumination on this relationship is studied in a statistical manner by deriving correlation coefficients of integral flux and absorption as a function of solar zenith angle limit, thus both an upper limit on the angle and the best correlated integral flux of protons are determined (energies in excess of 10 MeV). By considering the correlation of various energy ranges (from the GOES 8 differential proton flux channels) with CNA the range of proton energies for which the relationship between flux and absorption is best defined is established (15 to 44 MeV), thus confirming previous predictions about which proton energy ranges are most effective in giving rise to absorption during Polar Cap Absorption (PCA) events. An empirical relationship between the square root of the integral proton flux and the absorption, measured by the imaging riometer at Kilpisjärvi (IRIS), is determined and departures from linearity and possible causes are examined. Variations in spectral “hardness” and in collision frequency are demonstrated not to be significant causes of the observed departures from a linear relationship. Geomagnetic activity may be a significant factor in changing the relationship between the absorption and the square root of the integral proton flux, although it is concluded that the cause is likely to be more complex than a straightforward dependence on K_p . It is suggested that the most significant factor might be a bias in the absorption estimates imposed by the presence of Solar Radio Emission (SRE), which is not routinely measured at the operating frequency of IRIS, making its precise effect difficult to quantify. SRE is known to be most prevalent under conditions of high solar activity, such as those that might give rise to solar proton events.

Key words. Ionosphere (particle precipitation; solar radiation and cosmic ray effects; polar ionosphere)

Correspondence to: A. J. Kavanagh
(kavanagh@ucar.edu)

1 Introduction

Solar Proton Events (SPE), also known as Solar Energetic Particle (SEP) events, originate during active solar conditions, though arguments continue as to whether the particles are energised during the release of the X-ray flare or through acceleration by solar wind shock fronts driven by coronal mass ejections (Krucker and Lin, 2000). Regardless of which theory is correct, or whether it is some combination of the two, SPE are major (though relatively infrequent) space weather phenomena that can produce hazardous effects in the near-Earth space environment. Protons in the MeV energy range are the dominant species in SPE, although lower fluxes of heavier ions (e.g. He, Fe and O in various charge states) and electrons are also present. The ionospheric effects of SPE were first identified following the major event of 23 February 1956 (Bailey, 1957), when large signal losses on high-latitude VHF communication circuits were detected. The increased ionisation at low altitudes also resulted in the sudden disturbance of phase and amplitude on LF and VLF radio signals (Allen et al., 1957; Belrose et al., 1956; Ellison and Reid, 1956; Pierce, 1956). Around this time, Japanese researchers (Hakura et al., 1958) described polar cap effects observed before major geomagnetic storms based on observations of blackouts recorded by ionospheric sounding equipment.

Events similar to that of February 1956 were found to occur to the order of one per month. The protons gain access to the ionosphere through the polar caps and due to the high energies involved can cross closed field lines into the auroral zone; thus, these events became known as periods of Polar Cap Absorption (PCA) and the principal method of observing them is through the use of a riometer (Relative Ionospheric Opacity Meter using Extra-Terrestrial Electromagnetic Radiation), which measures the absorption of the cosmic radio noise at a given high frequency, usually between 20 and 60 MHz.

Since the cosmic noise absorption (CNA) is directly linked to the precipitating flux of solar protons, several workers have attempted to derive empirical relationships between the two parameters. Measurements of proton flux have been obtained through the use of rocket (Fichtel et al., 1963) and balloon instruments (Bailey, 1964) and compared with daytime observations of absorption at 30 MHz. In 1960 proton intensities greater than 30 MeV were measured by detectors on the Explorer 7 satellite and compared with data from 27.6 MHz riometers at College, Alaska and Thule (Van Allen et al., 1964). A relationship was derived linking the integral flux with the square of the absorption but the ratio of the two varied considerably during several events. Reid (1970) determined that the best correlation between integral fluxes and the CNA during the event of 5 February 1965 was for protons with energies in excess of 20 MeV. More complex methods have also been proposed, involving the derivation of proton flux spectra and the use of ionisation models (e.g. Adams and Masley, 1965). Juday and Adams (1969) determined that the ratio of integral flux to the squared absorption was least sensitive to model proton spectra for a threshold energy of 11 MeV. Potemra (1972) determined that the best relationship was obtained for a threshold energy of 7 MeV based on calculations from events in the period 1960 to 1967 and using power-law proton spectra. It was further concluded that the daytime polar cap absorption is most affected by 15 MeV protons, although a lack of differential flux measurements made this impossible to verify.

In this paper we return to the simple method of comparing the satellite integral fluxes with the cosmic noise absorption in the auroral zone to determine an empirical relationship between the two parameters with the aim of demonstrating how unreliable the technique can be without consideration of geomagnetic and, particularly, solar effects. Only daytime observations are used, since the complex chemistry of the D-region leads to significant electron depletion at night and the determination and implementation of recombination coefficients are beyond the scope of this work. The day/night dependence is illustrated by comparing the solar zenith angle with the correlation coefficient of the absorption and integral proton flux for a number of threshold angles. It is shown that an empirical relationship based on observed absorption is subject to severe constraints; in particular, the effects of high geomagnetic activity and solar radio emission (SRE) are shown to contaminate the empirical approach, leading to over- and underestimation of the absorption, respectively. It is concluded that any empirical method must be treated carefully and that suitable ionisation models should be employed to gain a more realistic measure of the PCA from satellite observations. Riometer observations of PCA during high solar activity must also be handled with care, since it is estimated that the observed signal can deviate from the true ionospheric absorption by a few decibels.

2 Theory and Instrumentation

2.1 Integral flux and absorption

Traditionally, auroral absorption is taken to occur at heights close to 90 km and is caused by the precipitation of electrons with energies in excess of a few keV. During PCA the majority of radio absorption occurs at lower altitudes due to the precipitation of high-energy solar protons (> 1 MeV). The atmospheric penetration of these particles is much greater than that of typical auroral electrons, with 100 MeV protons depositing energy at altitudes around 30 km (Reid, 1974). A relationship between a mono-energetic flux of particles and an ionisation profile in the atmosphere has been described by Rees (1989) and for a given particle energy the ion-electron production rate is proportional to the incident flux of charged particles.

The D-layer of the ionosphere can be represented as a Chapman alpha layer with an effective recombination coefficient that includes the attachment of electrons with neutral species to form negative ions, as well as the recombination with positive ions. In this case the production rate (and thus the flux) is proportional to the square of the electron concentration (e.g. Hargreaves, 1995). For slowly varying recombination rates CNA is approximately proportional to the height-integrated product of the electron density and the effective collision frequency (e.g. Hargreaves, 1969). By considering an integral flux of protons, which deposits across a range of altitudes, the height-integrated absorption is proportional to the square root of the flux as long as the collision frequency profile does not change rapidly with time and the absorption is observed on a constant frequency. If only daytime values are considered and the twilight transition is neglected, we implicitly assume a constant recombination coefficient. This approach mirrors the assumptions made by Patterson et al. (2001), who simplified the recombination coefficient into three cases: illuminated ionosphere, non-illuminated ionosphere and high altitudes (> 85 km).

2.2 Imaging Riometer for Ionospheric Studies (IRIS)

For this study CNA data have been taken from the Imaging Riometer for Ionospheric Studies (IRIS) at Kilpisjärvi, Finland (Browne et al., 1995), located in the auroral zone (69.05° N, 20.79° E geographic coordinates). Due to the configuration of the magnetosphere and the existence of the magnetotail, high-energy protons gain virtually uniform access to the polar cap (Reid and Sauer, 1967) and only the lowest energies are prevented from crossing closed field lines into the auroral zone. Thus, IRIS measures the vast majority of protons responsible for the PCA.

IRIS is operated by Lancaster University (UK) and has been recording data since September 1994. It is based on a design from the University of Maryland (Detrick and Rosenberg, 1990) and consists of a phased array of 64 dipole antennae that generate 49 (7×7) narrow beams. The whole array is sampled every second and data recording is arranged

such that each second is divided into eight time slots. The Kilpisjärvi IRIS uses the eighth time slot to record the output for a co-located wide beam antenna, with a beam width of $\approx 94^\circ$. This is similar to the design of the original and most common variety of riometer (Little and Leinbach, 1959), which uses a broad beam to monitor the cosmic radio noise. Since PCA events tend to be spatially uniform it is unnecessary to use a narrow beam of the riometer, which would be useful for distinguishing the absorption from narrow features (e.g. Collis et al., 1996); thus, the data presented in this paper come from the IRIS wide beam. However, the broad receiving beam pattern of these instruments leads to the detection of absorption from a range of angles from the zenith, leading to an overestimation of the true ionospheric absorption. Hargreaves and Detrick (2002) have developed corrections to the wide beam of IRIS that depend on the observed absorption; these have been applied to the data presented here.

Although the instrument records data every second, for this experiment these values have been averaged over 5 min since PCA tend to be slowly varying. The Kilpisjärvi IRIS has an advantage over riometers that have been used previously to develop empirical relationships with the proton flux, in that it operates at 38.2 MHz, which is a protected astronomy frequency, and so is theoretically resistant to contamination from HF transmitters.

Since the riometer actually monitors the level of cosmic noise, some measure of the background signal prior to attenuation is needed to account for the absorption. In the IRIS system this is accomplished by generating a “quiet-day-curve” (QDC) based upon at least 14 days of IRIS observations. The basic technique is described in Browne et al. (1995), although the algorithm has been modified somewhat to operate at the same resolution at which the instrument records data and to remove the bulk of the solar radio contributions from the QDC. The use of 14 days of data ensures that effects such as high snow levels and solar ionisation do not figure in the absorption output. Although the QDC can be computed to an accuracy of greater than 0.1 dB, caution must be used when applying it to periods of solar radio emission that can affect the position of the curve and so a cautious system error of ± 0.2 dB is often considered.

2.3 Geosynchronous Operational Environmental Satellites (GOES)

NOAA (National Oceanic and Atmospheric Administration) operates the Geosynchronous Operational Environmental Satellites (GOES), each of which carries a package of instruments designed to monitor space weather variations. Three principle measurements are made by the Space Environment Monitor (SEM) system: X-rays, energetic particles and magnetic fields. The observations presented in this paper are from the EP8 instrument on board the GOES-8 satellite, launched in 1995. This was the successor to the EPS (Energetic Particle Sensor) that flew on each of the previous GOES spacecraft. EP8 uses a series of solid-state detectors with pulse-height discrimination to measure proton,

Table 1. Corrected differential and integral proton flux channels from the EP8 instrument on board the GOES-8 satellite.

Channel	Differential (P) MeV	Integral (I) MeV
1	0.6–4.2	>1
2	4.2–8.7	>5
3	8.7–14.5	>10
4	15–44	>30
5	39–82	>50
6	84–200	>60
7	110–500	>100

alpha particle and electron fluxes. Proton data provided by NOAA are in two forms: integral and differential fluxes in seven energy channels (described in Table 1), all at 5-min resolution. In the differential channels the lowest energy threshold (P1) primarily responds to trapped outer-zone particles (energy >1 MeV); the P2 channel occasionally responds to trapped particles during magnetically disturbed periods. The higher channels respond only to the presence of solar protons. Throughout this paper, $J(>X)$ will be used to describe an integral flux of protons with a threshold energy, X, given in MeV.

Figure 1 displays the footprint of GOES-8, located in Northern Canada at 356.9° longitude AACGM (Altitude Adjusted Corrected Geomagnetic Coordinates - Baker and Wing, 1989) and on an L-shell of 6.85 Earth radii (R_E). Also shown is the field of view of the IRIS wide beam antenna at 104.3° and on an L-shell of $6.06 R_E$. Thus, IRIS and GOES-8 are separated by 107.4° of longitude and $0.79 R_E$ in L-shells ($\sim 1.5^\circ$ geomagnetic latitude). It is assumed that the incident solar protons bombard the atmosphere in a uniform manner such that the large separation between the two instruments is not important. This approach has been implemented previously when using the GOES satellites to provide measurement of the incident proton flux at the top of the ionosphere (e.g. Hall et al., 1992; Hargreaves et al., 1993; Hargreaves et al., 1987, and Collis and Rietveld, 1990). Similarly, IRIS is sufficiently poleward of the quiet time absolute cutoff boundary such that all but the least energetic (<1 MeV) protons will precipitate within the field of view (inferred from Leske et al., 2001).

3 Observations

3.1 Event identification

Polar Cap Absorption events are inherently linked to the flux of energetic solar protons incident on the ionosphere. The Space Environment Center (SEC) maintains a list of all solar proton events that have occurred since April 1976; the identification criterion is based upon a minimum integral flux of protons at geostationary orbit (i.e. the GOES spacecraft). Thus, a solar proton event is defined to occur only when the

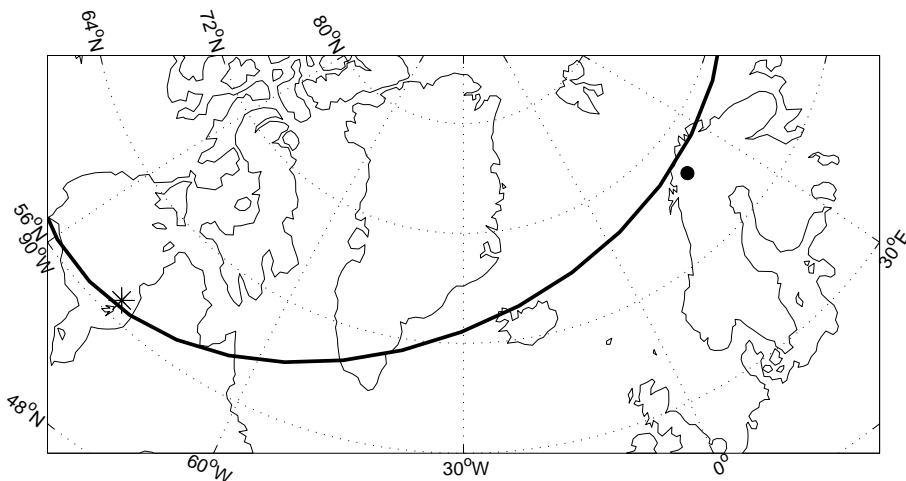


Fig. 1. Map displaying the position of the GOES 8 footprint (indicated by *) and the field of view of the IRIS wide beam riometer (at 90 km altitude). The footprint of $L=6.5$ is depicted as a thick black line demonstrating that the two instruments are on similar L shells. These are average values having been calculated for each year (from 1995 to 2001) using the International Geomagnetic Reference Field (IGRF) model.

flux of protons with energies above 10 MeV is greater than, or equal to, $10 \text{ cm}^{-2} \text{ s}^{-1} \text{ sr}^{-1}$ (p.f.u. - particle flux unit). In this study the data have been restricted to events that occurred between 1995 and 2001 inclusive, which cover the first seven years of IRIS operations. This leads to 51 separate events of varying duration, comprising over 90 days of solar proton observations. Table 2 lists the start and end times of the solar proton events together with their maximum p.f.u. as far as the authors are aware this is the largest database of events that has been used in a study of this kind.

In the next section two of the listed events are briefly presented. These have been selected because they demonstrate the general characteristics of PCA and SPE whilst showing how both geomagnetic and solar activity can influence the observed structure.

3.2 PCA/SPE examples

The top panel of Fig. 2 displays the solar proton flux in three integral channels (>10 , >30 and >100 MeV as described in the legend) from the SPE that began on 20 April 1998 (event 4 from Table 2). The middle panel displays the cosmic noise absorption (CNA) observed by IRIS at this time; the onset was at $\sim 14:00$ UT following a small negative deflection in the absorption that corresponded with a type II radio sweep, emitted at the same time as the X-ray flare and solar protons. Nighttime values are reduced due to the attachment of electrons to neutral species that occurs in the lower D-region during periods of darkness (Reid, 1974; Rietveld and Collis, 1993). The absorption varied slowly for the first two full PCA days, tracking the structure in the GOES proton data during daylight hours; this corresponded with quiet to unsettled geomagnetic activity ($K_p < 3$), as demonstrated in the bottom panel. For the majority of the fourth day (23 April) CNA was slowly varying except for a sharp negative spike from a type IV radio sweep that began at 05:38 UT and lasted until 06:20 UT. Towards the end of 23 April an interplanetary shock struck the magnetosphere leading to enhanced geomagnetic activity; K_p jumped from 1- to 5 as the absorption

became much more variable. Figure 3 shows event 42 from Table 2 in the same format as Fig. 2. This event began late on 24 September 2001 and lasted for 6 days. In contrast to the April 1998 event this PCA demonstrates more variability in the absorption signature. A number of negative spikes occur close to local noon on each of the days, suggesting enhanced solar radio emission. The absorption signature is more variable after 20:25 UT on 25 September, when a coronal mass ejection buffeted the magnetosphere, driving the K_p index up to 7+. Two more CME impacted the magnetosphere in this period (29 and 30 September).

These two isolated events demonstrate how variable the PCA signature can be between cases from a riometer located in the auroral zone. Electron precipitation following injection during substorms can lead to increased structure in the absorption, and solar radio emission can also lead to deviations from the signal due to the proton precipitation. The April 1998 PCA was generally free from magnetospheric contributions (at least from the 20–23 April), whereas the September 2001 event, which occurred closer to solar maximum, exhibited much greater contamination from both magnetospheric electrons and solar radio emission. Thus, it is apparent that when attempting to derive an empirical relationship between the proton flux and the cosmic noise absorption there are some constraints that must be considered. The most basic limit is the effect of solar illumination; for this study we are only interested in examining the daylight absorption and so all values that correspond to a dark ionosphere must be discarded.

3.3 Solar zenith angle

The solar illumination of the ionosphere plays an important role in the chemistry through both photodetachment of electrons and photodissociation of ions (e.g. del Pozo et al., 1999). This effect is most prominent at twilight as the Earth's shadow height increases/decreases, leading to a reduction/enhancement in the electron concentration (Collis and Rietveld, 1990). Thus, the solar zenith angle can be used

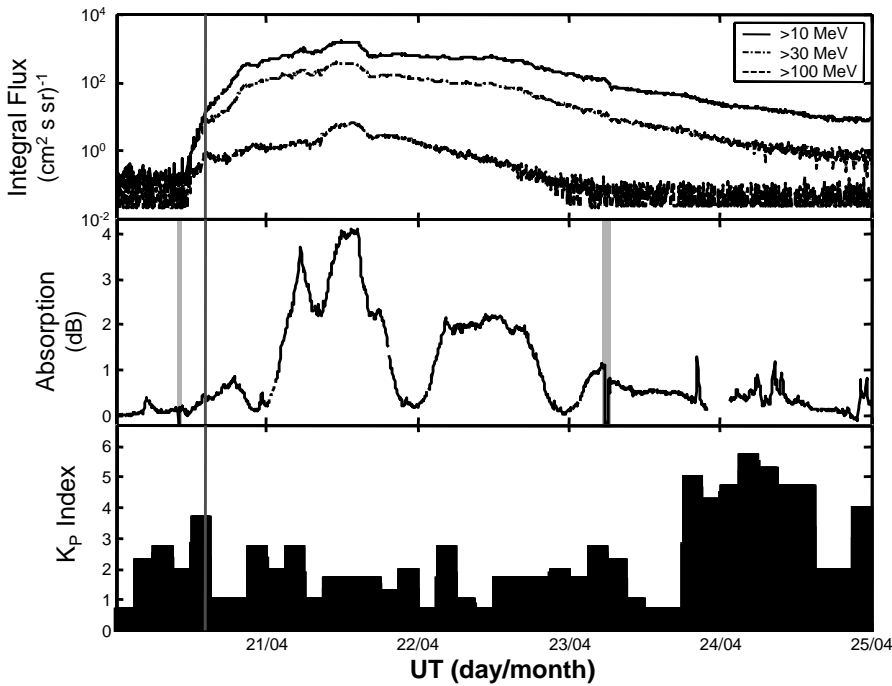


Fig. 2. Example of a PCA event from April 1998. The top panel shows the proton flux measured by GOES-8 in three integral energy channels. The middle panel displays the cosmic noise absorption measured by the IRIS wide beam riometer and the bottom panel shows the K_p index for the event. The start of the solar proton event is indicated by the vertical dotted line. Grey shading in the middle panel highlights periods of identified solar radio emission. Activity was generally low except for late on 23 April when a CME struck the magnetosphere; note the increased variability in the absorption following the impact compared with before.

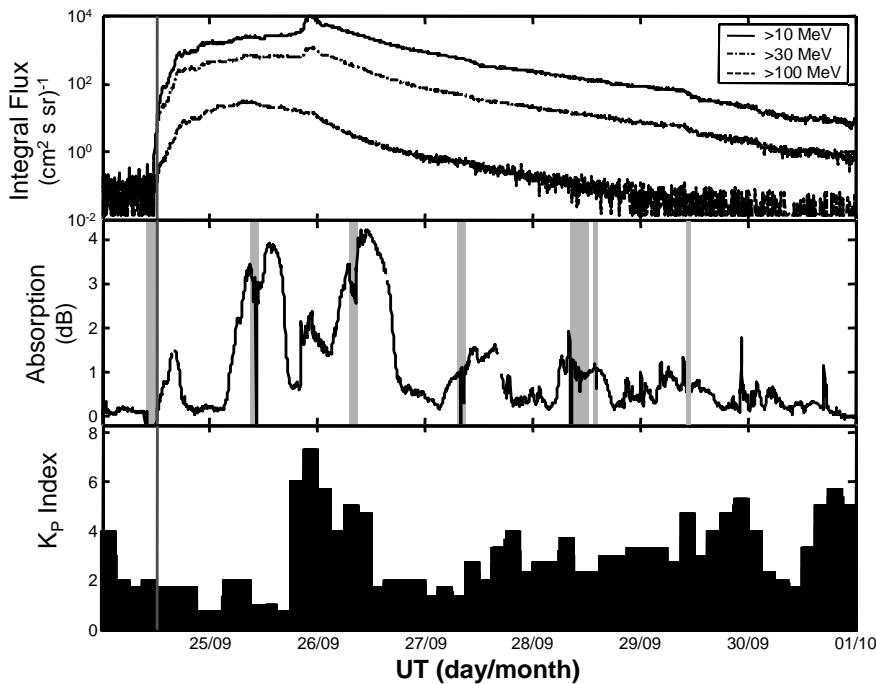


Fig. 3. Example of a PCA event from September 2001, in the same format as Fig. 2. Note the increase in K_p late on 25 September when a CME impacted the magnetosphere; this is reflected in the absorption data as a sharp rise shortly before midnight. At the same time the lower two energy channels from GOES-8 display increases in flux as the interplanetary shock accelerates the protons. Note that the absorption is more variable during this event, plus there are negative spikes and bays around local noon on each day.

as a proxy for the level of solar illumination and the effect that this has on the relationship between the proton flux and CNA can be explored.

Figure 4 displays the correlation coefficient (r) between the absorption and the integral proton flux for seven channels of the GOES 8 satellite from the combined data sets of the events listed in Table 2. This is presented as a function of a limiting solar zenith angle, χ_L , i.e. for each value of χ_L the correlation coefficient is calculated using data for all solar zenith angles below the limit; thus, the number of data

points that contribute to this varies from 1787 ($\chi_L=60^\circ$) to 20281 ($\chi_L=135^\circ$). At the lowest angle displayed it is clear that the absorption and the square root of the flux are well correlated for several channels; $J(>1)$ to $J(>50)$ all have $r>0.9$, whereas the two higher energy threshold channels have $r<0.9$ (~ 0.7 for $J(>100)$). During SPE $J(>10)$ can contain very energetic particles and so the slowly varying structure is reflected in the higher energy channels (e.g. the top panels of Figs. 2 and 3), though the signature may be different in the higher energy channels following acceleration

Table 2. All Solar Proton Events that contributed data to this study identified by number occurred since 1995 (first column). The second column lists the day and time when the integral proton flux (threshold of 10 MeV) rises above 10 p.f.u.. In the third column the end time and date of the event are indicated. The final column lists the maximum proton flux during the event.

	SPE onset: Date and time (UT)	SPE end: Day/time (UT)	Max. p.f.u
1	1995-10-20 08:25 UT	20/23:40 UT	63
2	1997-11-04 08:30 UT	05/13:40 UT	72
3	1997-11-06 13:05 UT	09/12:05 UT	490
4	1998-04-20 14:00 UT	24/15:50 UT	1700
5	1998-05-02 14:20 UT	04/03:35 UT	150
6	1998-05-06 08:45 UT	07/01:40 UT	210
7	1998-08-24 23:55 UT	29/12:10 UT	670
8	1998-09-25 00:10 UT	25/02:30 UT	44
9	1998-09-30 15:20 UT	02/08:30 UT	1200
10	1998-11-08 02:45 UT	08/02:45 UT	11
11	1998-11-14 08:10 UT	16/09:55 UT	310
12	1999-01-23 11:05 UT	23/16:45 UT	14
13	1999-04-24 18:04 UT	25/14:50 UT	32
14	1999-05-05 18:20 UT	06/05:50 UT	14
15	1999-06-02 02:45 UT	03/14:10 UT	48
16	1999-06-04 09:25 UT	05/05:15 UT	64
17	2000-02-18 11:30 UT	18/14:05 UT	13
18	2000-04-04 20:55 UT	06/01:55 UT	55
19	2000-06-07 13:35 UT	09/03:25 UT	84
20	2000-06-10 20:45 UT	11/11:30 UT	46
21	2000-07-14 10:45 UT	19/23:30 UT	24000
22	2000-07-22 13:20 UT	23/23:10 UT	17
23	2000-07-28 10:50 UT	28/13:10 UT	18
24	2000-08-11 16:50 UT	11/17:40 UT	17
25	2000-09-12 15:55 UT	15/21:40 UT	320
26	2000-10-16 11:25 UT	17/02:10 UT	15
27	2000-10-26 00:40 UT	26/10:00 UT	15
28	2000-11-08 23:50 UT	13/07:45 UT	14800
29	2000-11-24 15:20 UT	29/02:00 UT	942
30	2001-01-28 20:25 UT	30/00:35 UT	49
31	2001-02-29 16:35 UT	01/06:00 UT	35
32	2001-04-02 23:40 UT	06/13:40 UT	1100
33	2001-04-10 08:50 UT	13/10:55 UT	355
34	2001-04-15 14:10 UT	17/17:00 UT	951
35	2001-04-18 03:15 UT	20/08:20 UT	321
36	2001-04-28 04:30 UT	28/05:20 UT	57
37	2001-05-07 19:15 UT	08/17:30 UT	30
38	2001-06-15 17:50 UT	16/12:10 UT	26
39	2001-08-10 10:20 UT	10/14:40 UT	17
40	2001-08-16 01:35 UT	18/18:45 UT	493
41	2001-09-15 14:35 UT	15/15:45 UT	11
42	2001-09-24 12:15 UT	30/17:10 UT	12900
43	2001-10-01 11:45 UT	05/03:30 UT	2360
44	2001-10-19 22:25 UT	19/22:55 UT	11
45	2001-10-22 19:10 UT	23/01:15 UT	24
46	2001-11-04 17:05 UT	10/07:15 UT	31700
47	2001-11-19 12:30 UT	20/14:20 UT	34
48	2001-11-22 23:20 UT	27/21:00 UT	18900
49	2001-12-26 06:05 UT	28/10:45 UT	779
50	2001-12-29 05:10 UT	29/22:50 UT	76
51	2001-12-30 02:45 UT	04/23:55 UT	108

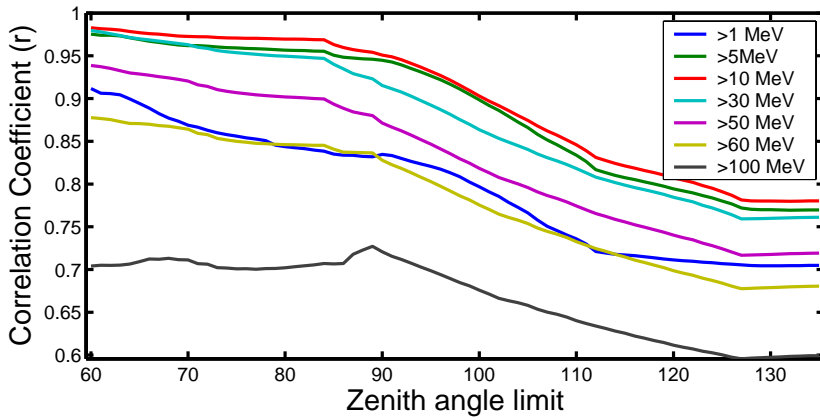


Fig. 4. The correlation coefficients (r) for 7 integral energy channels (from GOES-8) are displayed as a function of maximum solar zenith angle. The solar zenith angle limit describes the highest value for which riometer and satellite data have been used to determine the correlation coefficient. Therefore, each step in χ_L contains all data from the previous step.

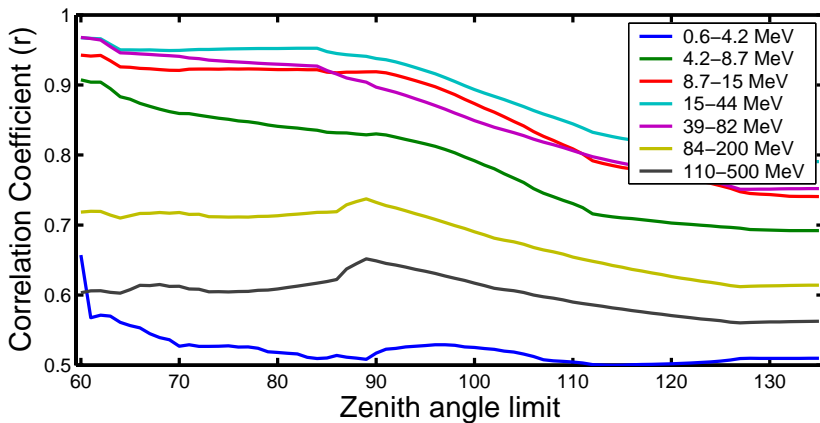


Fig. 5. In the same format as Fig. 4, however, now the differential flux channels from GOES-8 are used instead of the integral channels.

by a solar wind shock, as has occurred before midnight on 25 September 2001. $J(>100)$ has a lower correlation, since these particles are less likely to be responsible for the ionisation that leads to the absorption; this is demonstrated by those periods when $J(>100)$ is in the noise level, e.g. 23–24 April 1998 (Fig. 2). The lower correlation of the $J(>1)$ channel with the CNA may be attributed to too much variation; as stated in Sect. 2, this channel (I1 in Table 1) also contains geomagnetically trapped radiation which will display extra structure over the riometer observations, even though it will encompass the flux of solar protons.

$J(>10)$ has the best correlation with $J(>30)$ and $J(>5)$ close behind. The >10 MeV protons do not decrease in correlation by as much as the other energy channels (except $J(>100)$), until $\chi_L=84^\circ$ at which time the rate of decorrelation increases; throughout, those protons with energies in excess of 10 MeV correlate best with the absorption and we can infer that the range of proton energies that contribute most effectively to the observed absorption is within 10 and 50 MeV. A better estimate of the energy of the protons most responsible for the PCA can be obtained by considering the differential proton fluxes and how well they correlate with the CNA.

Figure 5 presents correlation curves for the differential flux of protons against the solar zenith angle limit; the energy range for each channel is included in the legend and listed in Table 1. Two of the GOES channels, covering an energy range of 15–82 MeV, exhibit $r > 0.95$ at a zenith angle of 60° . Protons with energy in the range of 15–44 MeV retain a higher correlation as the solar zenith angle limit increases, whereas the 39–82 MeV channel decorrelates at a higher rate, especially after $\chi_L=84^\circ$. Modelling the spectrum of precipitation (possibly using a power law to link the channels) may make it possible to narrow the energy range, though results would depend heavily on the assumptions made in generating the spectrum.

It appears that data from below $\sim 84^\circ$ solar zenith angle can be used in the formation of an empirical relationship between the CNA at 38.2 MHz and the integral proton flux. The best threshold energy for the protons is 10 MeV, which is in broad agreement with the results of Juday and Adams (1969) (11 MeV) and Potemra (1972) (7 MeV). Similarly, the best correlation with the differential fluxes of protons is for the energy range of 15–44 MeV and Potemra (1972) speculated that 15 MeV protons were most responsible for the absorption. The current findings would seem to support this. Having established some of the limits on the proton contribution

to polar cap absorption it is possible to attempt to fit a function to the riometer and particle sensor data. Since those times when photo detachment affects the absorption can now be removed the resulting relationship can be used to probe the effects of both the geomagnetic and solar activity on the lower ionosphere during solar proton events.

4 Flux – Absorption Relationship

In the following derivation of an empirical relationship between the proton flux and CNA, we concentrate on the integral flux of protons above 10 MeV, which precipitate throughout the altitude range of the absorbing region.

The long duration observations of both IRIS and GOES provide a large database for determining the absorption-flux relationship. By using a geosynchronous satellite, continuous observations of proton fluxes are possible during the entire duration of a Solar Proton Event, rather than being limited to the polar passes of an orbiting spacecraft (usually in 90 minute orbits). It is assumed that the separation of the instruments (~ 8 h of MLT) should not adversely affect the results, as explained in Sect 2.3.

Section 2.1 described how the CNA should vary with the square root of the integral flux (e.g. Van Allen et al., 1964; Reid, 1970; Potemra, 1972). In this case a relationship of the form:

$$A = m\sqrt{J(>10)} + c \quad (1)$$

is fitted to our results, where A is the absorption in decibels, $J(>10)$ is the integral flux of protons with energy greater than 10 MeV ($\text{cm}^{-2}\text{s}^{-1}\text{sr}^{-1}$), and m and c represent gradient and intercept, respectively.

Figure 6 displays the scatter of absorption with the square root of the >10 MeV integral flux (top panel). The line of best fit is also displayed, and the values for m and c are 0.074 and 0.067, respectively. All levels of K_p have been included in the fit, but only absorption values from periods with a solar zenith angle of less than 80° have been included. This safely removes the sudden change in correlation observed in Fig. 4 and results in a correlation coefficient of 0.975. An intercept of zero ($c=0$) would represent the ideal case, in which the GOES sensors measured no proton flux and the riometer recorded no absorption. The method of determining the absorption for IRIS through quiet-day curve generation leads to a negligible contribution from solar illumination. Error margins have been calculated for the fit to the data through a least-squares method and yield a median correction of ± 0.376 dB (the maximum was ± 0.377 dB); this overlaps the ideal value of 0 dB for $\sqrt{J(>10)}=0$.

The bottom panel of Fig. 6 plots the residuals (observed minus calculated absorption) and for a good fit to the data these should be scattered evenly around zero with no trends. This is reasonably true below $\sqrt{J}=20$, with the bulk of the scatter ($\sim 90\%$) within ± 1 dB. After $\sqrt{J}=60$ there is a distinct trend from high to low values in the data, with most scatter located between 0 and 3 dB before $\sqrt{J}=100$, and between

0 and -3 dB after that. Thus, even though the correlation is high, there are still problems with the linear relationship. At higher flux levels the absorption is overestimated by as much as 4 dB and likewise the absorption is underestimated at the mid flux range. In the next section we discuss possible explanations for this problem and examine the effect of removing data from geomagnetically active periods.

5 Discussion

So far, it has been demonstrated that for the polar cap absorption and solar proton events between 1995 and 2001, there is an excellent correlation between the square root of the integral flux of >10 MeV protons with the cosmic noise absorption observed in the auroral zone. The correlation is best when data for solar zenith angles greater than $\sim 80^\circ$ are excluded (Fig. 4). Around 84° there is a sudden decrease that is possibly related to the effects of the sunrise transition when there is a delay in the build-up of atomic oxygen that Collis and Rietveld (1990) linked to the rate of electron detachment through reactions with both ionic ozone and CO_3^- . Since all twilight values contribute to the correlation calculation r does not decrease as much as it might for just sunrise. The increasing rate of change in the decorrelation observed after 90° is linked to the movement of the Earth's shadow height upward through the ionosphere as oxygen is rapidly depleted and photodetachment of electrons can no longer take place (Reid, 1974; Collis and Rietveld, 1990).

Although initially promising with a high correlation ($r=0.975$), the fit of the square root of the flux to the CNA (Fig. 6) leads to a wide spread of residuals and distinct trends at the higher flux values. One parameter that may upset the computation is the effective collision frequency, which so far has been assumed to remain relatively constant in time at all altitudes. The electron-neutral collision frequency is the dominant factor in determining ionospheric absorption. It depends on two factors: the concentration of the various atmospheric constituents and the temperature of the electrons (Schunk and Nagy, 1978; 1980). The neutral density and collision frequency increase exponentially with decreasing altitude. As a result, electrons become thermalized; at lower altitudes the temperature of the electrons is considered equal to that of the neutral species but if this is not the case, then collisions will increase, in turn affecting the absorption. Frictional heating leads to an increase in ion temperature, but the ion-electron collision frequency has only a small role in the effective collision frequency at heights where radio absorption is appreciable. The electron temperature increase during frictional heating is significantly lower in the F- and E-layers (Schlegel and St.-Maurice, 1981) but does become comparable in the D-layer. Stauning (1984) determined that strong electric fields in the polar cap (invariant latitude= 77°) could raise the E-region electron temperature sufficiently to produce additional absorption of 0.5 dB on a 30 MHz riometer. For IRIS (operating at 38.2 MHz) this translates to a maximum increase of ~ 0.3 dB which is well within the error

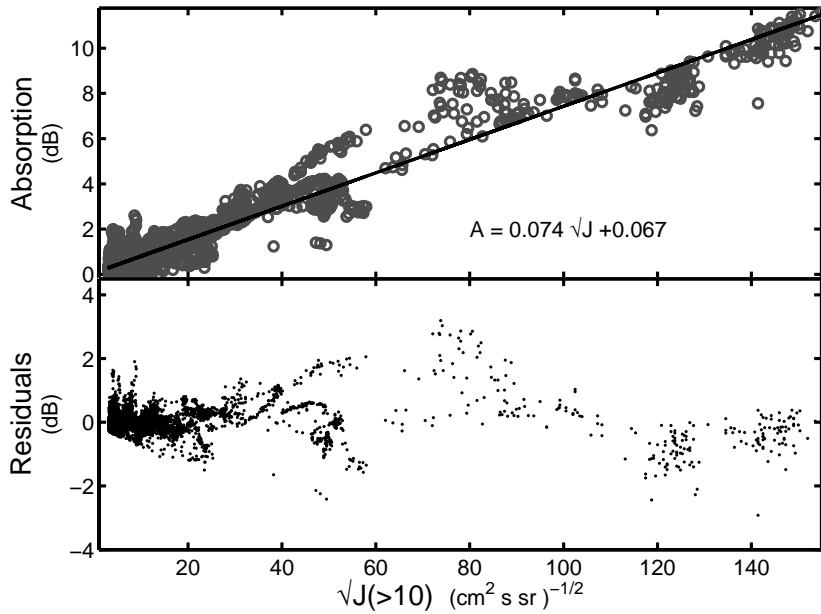


Fig. 6. Linear fit between the square root of the >10 MeV integral flux ($J(>10)$) and the CNA from the wide beam riometer. The top panel displays the scatter of the points and line of best fit; the coefficients of the fit are displayed. The bottom panel presents the residuals (Observed minus calculated absorption) as a function of the square root of $J(>10)$. Note the trends at higher flux values. The correlation coefficient between the two fitted parameters is 0.975.

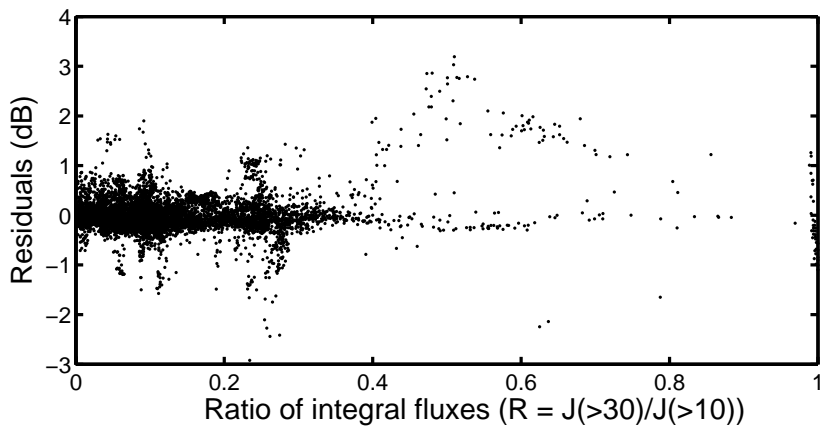


Fig. 7. Residuals of the fit plotted as a function of the ratio: $R=J(>30)$ to $J(>10)$. R provides a simple indication of the hardness of the spectrum of precipitation by determining how much of the >10 MeV protons are also >30 MeV. A spread of absorption lies below $R=0.3$; the bulk of the residuals are between ± 1 dB ($\approx 85\%$). There is no readily apparent trend in the residuals that suggests consistently higher errors at larger values of R .

estimate. Thus, it is not expected that increased collision frequency would lead to dramatic changes in the flux-absorption relationship.

The collision frequency may still play an important role due to the varying deposition of the solar protons in different events. The following section investigates how CNA resulting from a “hard” spectrum of precipitation differs from that due to a less energetic shower of protons.

5.1 Spectral hardness

For comparable electron densities the cosmic noise absorption is greater at lower altitudes due to the effects of the electron-neutral collision frequency. This may have a significant effect on the derived relationship when the spectrum of proton precipitation varies significantly; either during an event or between one event and the next. A “hard” spectrum of precipitation during SPE results in energy deposition at

lower altitudes (30–50 km). Whilst resulting in lower electron concentrations this could still lead to higher integral absorption; i.e. although the “softer” protons occur in greater fluxes and produce more ionisation, the more energetic protons will still provide a considerable contribution to the absorption.

To test the dependence of CNA on the spectrum of proton precipitation, Fig. 7 plots the residuals of the empirical fit as a function of the ratio, R , of $J(>30)$ to $J(>10)$; there are few examples of the proton flux being composed of predominantly >30 MeV particles ($\sim 2\%$ with a ratio >0.5). As R approaches 1 there is a spread of absorption (± 1.3 dB) but there are few data points to draw meaningful conclusions ($\sim 0.5\%$). Most of the data lies below $R=0.3$ ($\sim 94\%$) and these points spread between ± 1 dB with a few extending to ± 3 dB. There is no discernable trend in the data to suggest that the hardness of the spectrum has more than a very minor role in affecting the flux-absorption relationship. There are

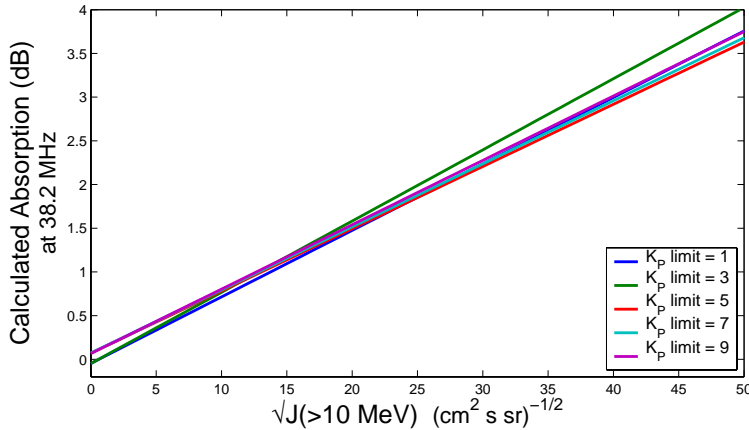


Fig. 8. Flux-absorption relationship calculated for various upper limits of K_p . Note the increase away from zero intercept for higher K_p . Overall, the gradient drops between $K_p=3$ and 9, however, the gradient rises from $K_p=1$ and from $K_p=5$. The values of the coefficients are displayed in Table 3.

two other possible factors that could cause the observed variation of the CNA: increased geomagnetic activity and solar radio emission. The following sections examine these, and explain how they might cause the measured absorption to be different from that caused only by solar protons.

5.2 Geomagnetic activity

We have used the planetary K index as our proxy for geomagnetic activity. Since only daytime values are included in the flux-absorption relationship, the magnetospheric precipitation that we anticipate is from electrons that have drifted following injection during substorms. As such, the precipitation is likely to be more dependent on the night-side activity rather than on the local level. Relationships between absorption and K_p have already been determined (e.g. Hargreaves, 1966; Kavanagh et al; 2003), whereas links between local geomagnetic indicators and absorption are less well defined, with known results being station specific (e.g. Oguti, 1963).

The results plotted in both Figs. 4 and 6 contained data from all levels of geomagnetic activity, as defined by the K_p index. This did not seem to effect the correlation. During the most active periods, however, there is a general tendency for absorption to increase due to elevated precipitation of energetic electrons (e.g. energy >10 keV). The nature of CNA as measured through the riometry technique is such that the contributions of high-energy protons and electrons are cumulative. In general, the electron contribution is likely to be a small percentage of the total absorption from the solar proton ionisation, but at times it could contribute as much as 6 dB (e.g. Nielsen and Honary, 2000), though cases of such high absorption are rare. Electron induced absorption has a broad peak on the dayside of the ionosphere (Kavanagh et al., 2003 and references therein) in the post dawn sector (06:00–12:00 MLT); thus, electron precipitation would lead to contamination of the flux-absorption relationship by creating higher levels of absorption than the proton flux alone would warrant.

To investigate the effect of geomagnetic activity on the empirical relationship, a number of threshold values of K_p

were used to limit the data. Only those data for which K_p was less than the threshold value were then fitted, using a linear relationship with the form of Eq. (1). Table 3 presents the gradient (m) and intercept (c) for 9 values of K_p . Also included are the corresponding correlation coefficients and an associated error level in the absorption, derived from a least-squares fitting technique. The final column provides the number of data points that contributed to the fit. Figure 8 plots several of these lines (as indicated in the legend) for $J(>10)$ from zero to $2500 \text{ cm}^{-2} \text{ s}^{-1} \text{ sr}^{-1}$.

Differences in the parameters are small, suggesting that K_p has no clear systematic effect on the relationship. A separation in the value of the intercept occurs between $K_p=4$ and $K_p=5$, leading to higher values for the larger K_p indices. This would be expected if electron precipitation is contributing to the observed absorption that determines the relationship. High K_p during PCA is often indicative of geomagnetic storm conditions following the impact of a CME associated with the SPE. Often this leads to acceleration of the solar protons resulting in higher fluxes. Thus, one might expect to see a higher gradient for higher K_p , however, this is not the case with the gradient diminishing after $K_p=4$, suggesting that some other factor is involved in reducing the observed absorption. This is possibly solar radio emission (SRE), which causes the observed absorption to deviate from the true level by enhancing the radio signal at the riometer frequency. The following section explains the problems of solar radio emission and examines four different PCA events in an attempt to determine whether SRE is a likely candidate for affecting the empirical relationship.

5.3 Solar Radio Emission (SRE)

The riometry technique is a relatively simple method of probing the lower ionosphere and its ability to monitor during daylight hours is an improvement over many current optical techniques; however, there is a severe constraint on the use of daytime CNA observations, particularly close to solar maximum. At this time the Sun is more active in the emission of radio waves, as demonstrated in Sect. 3.2, where the PCA

Table 3. Parameters of fits to the CNA and integral flux using the form: $A=m\sqrt{J(>10)}+c$. Columns left to right display the maximum K_p of the data used, the gradient of the fit, the intercept, the correlation coefficient, least-squares fit error and the number of points used.

max. K_p	m (dB/(cm ² s sr) ^{1/2})	c (dB)	r	ΔA (dB)	# of points
1	0.076	-0.046	0.972	± 0.211	1402
2	0.082	-0.069	0.964	± 0.243	3230
3	0.081	-0.047	0.953	± 0.249	4557
4	0.076	+0.012	0.960	± 0.286	5279
5	0.071	+0.071	0.969	± 0.331	6169
6	0.071	+0.079	0.967	± 0.335	6481
7	0.072	+0.073	0.967	± 0.345	6813
8	0.074	+0.068	0.971	± 0.375	6964
9	0.074	+0.067	0.974	± 0.376	7022

close to solar maximum suffered perceptible contamination from SRE (Fig. 3). SPE and consequently PCA are most common close to the maximum of the solar cycle (Shea and Smart, 2002), and the solar flares that lead to SPE are themselves often accompanied by radio bursts and noise storms that reduce the amount of observed absorption from the true level in the ionosphere (e.g. Ranta et al., 1993). Thirty-six of the 51 events used in this study occurred in 2000–2001, across the solar maximum. Figure 3 (bottom panel) showed that on many of the days of the September 2001 event, a negative spike appeared in the riometer data close to local noon. At these times the apparent position of the Sun in the sky is within the receiving beam of the riometer, and the wide aperture ($\sim 94^\circ$ to the half power point) ensures that solar radio emission is recorded, resulting in unrealistic negative absorption and sometimes leading to saturation of the receiver. A further complication arises when the CNA is high (as is often the case during polar cap absorption); when solar emission occurs the observed absorption may not drop below zero, making it difficult to estimate when the observations deviate from the true ionospheric cosmic noise absorption. It might be argued that through the use of a narrow beam riometer this effect can be reduced (if not removed altogether), unfortunately the radio emission is often so strong that the side lobes of the riometer beam (although less sensitive than the main beam) will be contaminated by the SRE and, therefore, affect the overall riometer signal (Kavanagh, 2002). A similar problem occurs using riometers deeper in the polar cap, even when the main beam is not pointing towards the Sun although the effect would probably be reduced.

Figure 9 presents the results of determining a flux-absorption relationship for four separate events, in each case with a zenith angle limit of 80° but with no restriction on the level of geomagnetic activity. Two of the lines are from the PCA/SPE described in Sect. 3; the solid line is for the April 1998 PCA and the dashed line is for the event in September 2001. The remaining events are from 2–6 April 2001 (dash-dot) and 14–19 July 2000 (dotted) - the so-called Bastille Day event. Table 4 lists the parameters of the fit and also lists the median K_p for the events, as well as two indicators

of the level of solar activity: the median sunspot number and the $f_{10.7}$ index for each event. The minimum number of data points used to generate the fits was 439 for April 2001, whereas the maximum number was for the Bastille Day event (965).

The intercepts closest to zero occur for the PCA events of April 1998 and July 2000 but the errors associated with the fitted relationships for these two days are distinctly different. In April 1998 the median error was over three times smaller than for July 2000. The two 2001 events also have similar intercepts but their associated errors are separated by ~ 0.1 dB. These two events had a similar level of geomagnetic activity throughout but the September event demonstrates a much shallower gradient, very similar to the Bastille Day. Thus, the events with higher geomagnetic activity lead to lower absorption for higher fluxes than when activity is quiet to moderate. Interestingly, two events of similar activity display very different gradients (over 1 dB difference for $J(>10)=3600$ p.f.u), and two events with quite different levels of geomagnetic activity have very similar gradients. The Bastille Day event peaked at $K_p=9$ for daytime activity compared with $K_p=5$ for the September 2001 event.

In summary, there appears to be no clear relationship between the level of geomagnetic activity and the gradient of the fitted curve. To some extent, it is obvious that one should not expect a direct relationship between a rapidly varying quantity such as absorption and a discrete activity index such as K_p . Kavanagh et al. (2003) demonstrated that, although a statistical relationship could be applied over long time scales, very significant variations in local absorption levels could occur while the global K_p index remained constant.

These differences in behaviour between apparently similar days can perhaps be better understood when the level of solar radio emission (SRE) is taken into account. During the April 1998 event (shown in Fig. 2), there was little contamination of the riometer measurements by SRE. The riometer measurements made during the PCA event of September 2001, however, exhibited a number of spikes and bays around local noon (Fig. 3), and it is therefore inferred that the level of SRE was high. The possibility therefore exists that the actual

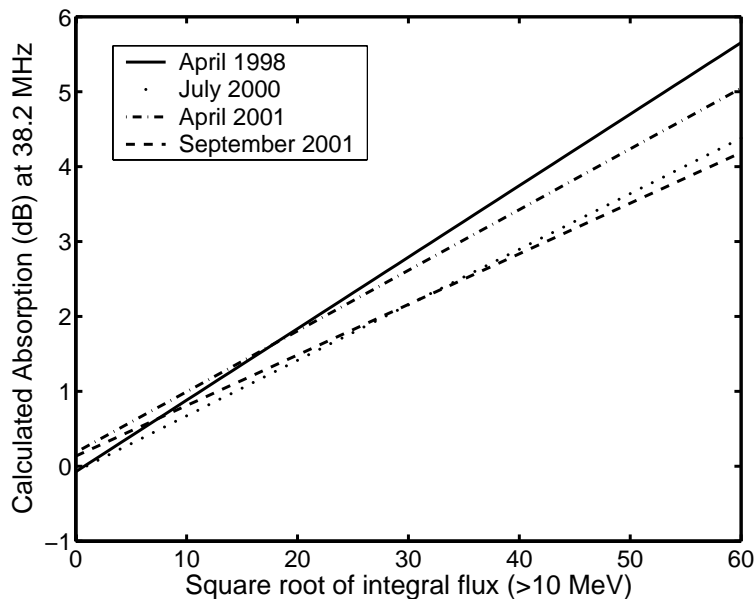


Fig. 9. Flux-absorption relationship calculated for four separate PCA/SPE. Coefficients of the fit are displayed in Table 4. Both April 2001 and September 2001 had similar geomagnetic activity levels, however, the Sun was more active during September 2001; thus, the gradient is shallower due to more contamination from solar radio emission. Higher activity during the July 2000 event cannot compensate for the increased SRE contamination.

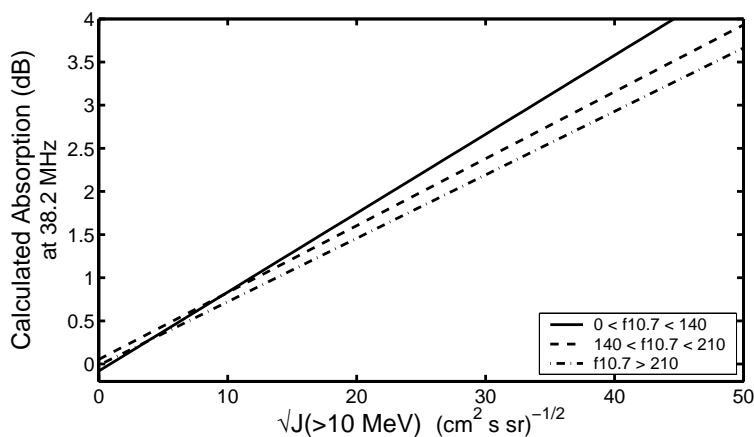


Fig. 10. Three lines are displayed depicting the relationship between the integral proton flux and the cosmic noise absorption calculated for three ranges of solar activity defined by the $f10.7$ index. Note that with higher activity the absorption reduces (for $\sqrt{J} > 10$) due to a combination of reduced gradient and intercept (for the two higher ranges).

absorption levels in the September 2001 event were significantly higher than those measured by the riometer, as the presence of SRE would increase the received signal level, thereby decreasing the calculated absorption. For the PCA events of July 2000 and April 2001 geomagnetic activity was also significant, and the actual levels of absorption may thus have been higher than that measured by the riometer, due to SRE contamination.

The dramatic extent to which SRE can affect absorption measurements can be seen in Fig. 3. On 25 September 2001, a large spike-like event occurred, which reduced the absorption level almost instantaneously from some 3 dB to near zero. This variation was almost certainly due to a burst of SRE. It is instructive to compare this event to the sharp increase in absorption (~ 1.3 dB), which occurred on the following day in response to a sudden storm commencement. Thus, it seems that the effect of SRE on absorption can easily be double that caused by geomagnetic activity, and has the opposite sense.

It is important to note that even though we use the $f10.7$ and sunspot numbers as indicators of the level of solar activity, the authors are unaware of any published study linking these parameters directly to the solar radio emission at 38.2 MHz. Some evidence does exist linking the duration of SRE (as a percentage of the day) as observed by a riometer, with the $f10.7$ flux and with the duration of X-ray emission above a threshold, and this will be the subject of a future investigation using IRIS observations during periods of low precipitation. Figure 10 displays the flux-absorption relationship derived under three different levels of solar activity, as derived from the $f10.7$ index. Higher solar activity leads to a drop in the calculated absorption from the same integral flux except at relatively low PFU. This reduction is achieved through decreases in the derived gradient, as well as, in the intercept values for the two higher activity bins. The associated error of the relationship from highest solar activity (± 0.54 dB) is more than double those of the first two bins (± 0.27 dB). Thus, on a qualitative level the increased solar

Table 4. Parameters related to the fit of absorption to the square root of the integral proton flux for the four events depicted in Fig. 9. These include (left to right) the gradient, m , intercept, c , median associated error, ΔA , and three indices of the geomagnetic (K_p) and solar ($f10.7$ cm flux and sunspot number) activity.

	m (dB/(cm ² s sr) ^{1/2})	c (dB)	ΔA (dB)	Median K_p	Median $f10.7$ number	Median Sunspot number
April 1998	0.096	-0.074	± 0.212	2- (1.7)	91	38
July 2000	0.074	-0.070	± 0.673	4- (3.7)	223	302
April 2001	0.081	+0.185	± 0.326	2+ (2.3)	210	217
September 2001	0.068	+0.135	± 0.409	3- (2.7)	270	278

activity can be shown to reduce the empirical flux-absorption relationship through reduction of the observed absorption. Due to the daily nature of the $f10.7$ index and the relatively low amount of corresponding PCA data that is available, it is impossible to quantify the effect of SRE at this stage, although it is clear that SRE does lead to contamination of CNA during solar active periods.

A possible consequence of the effect of solar radio emission during PCA is false observations of the midday recovery. This phenomenon was first described and defined by Leinbach (1961, 1967) and consists of a decrease in CNA observed near the edge of the cut-off boundary around noon. Satellite measurements of the precipitation of energetic particles have confirmed the existence of this effect as a combination of a local reduction in cut-off latitude (e.g. Reid and Sauer, 1967) and the development of an anisotropy in the pitch angle distribution (e.g. Paulikas et al., 1968). However, equatorward riometers are likely to be more susceptible to SRE due to the relative position of the Sun in the sky, maximising around local noon, thereby either enhancing the effect or indeed producing a false observation of a midday recovery. Although this is speculation, the effect of solar radio emission on cosmic noise absorption measurements is such that it seems likely that some observations of midday recoveries are in fact an effect of increased solar radio signal at the riometer operating frequency. Comparisons of riometers close to the absorption cut-off boundary and deeper in the polar cap may determine whether this could be an effect of SRE since one would expect the solar emission to still affect the poleward riometer measurement (to a lesser degree) whereas a true recovery should be confined to the equatorward observations.

6 Summary and Conclusions

The relationship between cosmic noise absorption and solar proton bombardment has been investigated using 51 separate solar proton events of varying duration and intensity. As far as the authors are aware, this is the largest database used in a study of this nature. This paper highlights the excellent correlation that exists between high-energy protons (>10 MeV) and cosmic radio noise absorption in the auroral zone during solar proton events. The correlation is heavily dependent on

the solar zenith angle due to chemical changes in the lower, unilluminated D-region, and data corresponding to zenith angles smaller than $\sim 80^\circ$ show only small changes in correlation coefficient. Our results indicate that the integral flux most responsible for PCA has an energy threshold of 10 MeV and furthermore, we identify the most responsible protons as having energy in the range of 15 to 44 MeV. These findings confirm the results of previous authors. Although there is an excellent correlation between the flux and absorption ($r=0.975$) some serious underlying problems with the linear fit to the data have been discovered. The calculated and measured absorption levels can differ by as much as 3 dB, although it must be remembered that in some cases short-term additional electron precipitation may result in higher than expected absorption. It appears that increased geomagnetic activity (as indicated by the K_p index) does not seem to affect the overall correlation. We have demonstrated that SRE plays a large role in contaminating the measured absorption and reducing it from the true value. In turn, this effects the derivation of a flux-absorption relationship, leading to an underestimation of absorption. This is shown to dominate over the geomagnetic effects by comparing four different PCA with different magnetospheric conditions (as described by the median K_p) and solar activity (defined by the average $f10.7$ cm index and sunspot number for the event). The event with least geomagnetic and solar activity resulted in the smallest associated error (± 0.211 dB), whereas the event with highest sunspot number and K_p recorded the highest error (± 0.673 dB).

Comparing relationships derived using data corresponding to different levels of solar activity demonstrates a trend of lower absorption levels occurring for similar integral proton flux at higher $f10.7$ values. This reinforces that SRE has a distinct effect on the CNA during solar active conditions, although it is difficult to quantify this effect with the current data set. Since many SPE occur during the active phase of the solar cycle, any attempt to derive or utilize an empirical relationship must be treated with utmost care due to the effects of SRE. More thorough methods, in which the observed spectrum of precipitation is used to model the absorption, are also limited by uncertainties in D-region recombination rates, although steps toward resolving these problems have been undertaken by Hargreaves et al. (1987, 1993).

The current study highlights an even more significant problem, namely the difficulty in measuring the true ionospheric absorption level when riometer data are affected by SRE. Under these conditions comparisons between modelled results and observations might suggest that the modelling is flawed, when in fact it is the riometer data that is misrepresenting the ionospheric conditions. Further work on understanding the extent and magnitude of solar radio emission in riometer measurements is much needed and an ability to determine and remove the effects would improve the data tremendously. This is the subject of an ongoing study using periods of low absorption from IRIS in comparison with solar indices.

Acknowledgements. The Imaging Riometer for Ionospheric Studies (IRIS) is operated by the Department of Communication Systems at Lancaster University (UK), funded as a UK National facility by the Particle Physics and Astronomy Research Council (PPARC) in collaboration with the Sodankyl Geophysical Observatory (SGO). The GOES data were obtained through the Space Physics Interactive Data Resource (SPIDR) from the National Geophysical Data Center (NGDC), part of NOAA (National Oceanic and Atmospheric Administration). Preliminary listings of the solar proton events were obtained from the Space Environment Center (NOAA), (www.sec.noaa.gov/alerts/SPE.html) as were the $f_{10.7}$ index and sunspot numbers. Geomagnetic index data were provided by the WDC for Geomagnetism, Kyoto, Japan. We gratefully acknowledge M. Grill (Lancaster) for providing information on the side lobes of IRIS. AJK is indebted to PPARC and the Rutherford Appleton Laboratories for a CASE research studentship during which part of this work was completed at Lancaster University. AJK would also like to thank HAO/NCAR/NSF for providing a postdoctoral research fellowship. We thank the referees for useful comments and criticisms.

Topical Editor M. Lester thanks J. Manninen and another referee for their help in evaluating this paper.

References

- Adams, G. W. and Masley, A. J.: Production rates and electron densities in the lower ionosphere due to solar cosmic rays, *J. Atmos. Terr. Phys.*, 27, 289–298, 1965.
- Allen, A. H., Crombie, D. D., and Penton, W. A.: Long-path V.L.F.-Frequency variations associated with the solar flare of 23 February 1956, *J. Atmos. Terr. Phys.*, 10, 110–113, 1957.
- Bailey, D.K.: Disturbances in the lower ionosphere observed at VHF following the solar flare of 23 February 1956 with particular reference to the auroral zone absorption, *J. Geophys. Res.*, 62, 431–463, 1957.
- Bailey, D. K.: Polar Cap Absorption, *Planet. Space Sci.*, 12, 495–541, 1964.
- Baker, K. B. and Wing, S.: A new magnetic coordinate system for conjugate studies at high latitudes, *J. Geophys. Res.*, 94, 9139–9143, 1989.
- Belrose, J. S., Devenport, M. H. and Weekes, K.: Some unusual radio observations made in 23 February 1956, *J. Atmos. Terr. Phys.*, 8, 281–286, 1956.
- Browne, S., Hargreaves, J. K., and Honary, B.: An Imaging Riometer for Ionospheric Studies, *Elect. Comm. Eng. J.*, 7, 209–217, 1995.
- Collis, P. N., and Rietveld, M. T.: Mesospheric observations with the EISCAT UHF radar during polar cap absorption events: 1. Electron densities and negative ions. *Ann. Geophys.*, 8, 809–824, 1990.
- Collis, P. N., Hargreaves, J. K., and White, G. P.: A localised co-rotating auroral absorption event observed near noon using imaging riometer and EISCAT, *Ann. Geophys.*, 14, 1305–1316, 1996.
- del Pozo, C. F., Turunen, E., and Ulich, T.: Negative ions in the auroral mesosphere during a PCA event around sunset, *Ann. Geophys.*, 17, 782–793, 1999.
- Detrick, D. L. and Rosenberg, T. J.: A Phased-Array Radio wave Imager for Studies of Cosmic Noise Absorption, *Radio Sci.*, 25, 325–338, 1990.
- Ellison, M.A. and Reid, J.H.: A long-wave anomaly associated with the arrival of cosmic-ray particles of solar origin on 23 February 1956, *J. Atmos. Terr. Phys.*, 8, 291–293, 1956.
- Fichtel, C. E., Guss, D. E., and Ogilvie, K. W.: Details of individual solar particle events, in: *Solar Proton Manual*, edited by McDonald, F. B., NASA Tech. Rep. TRR-169, 19–56, 1963.
- Hakura, Y., Takenoshita, Y. and Otusuki, T.: Polar blackouts associated with severe geomagnetic storms on Sept. 13th 1957 and Feb. 11th 1958, *Rep. Ionosph. Res. In. Japan*, 12, 459–467, 1958.
- Hall, C., Brekke, A., van Eyken, A. P., Hoppe, U.P., and Thrane, E. V.: Incoherent Scatter Radar Observations of the middle atmospheric response to a PCA, *Adv. Space. Sci.*, 12, 10 289–10 294, 1992.
- Hargreaves, J. K.: On the variation of auroral radio absorption with geomagnetic activity, *Planet. Space Sci.*, 14, 991–1006, 1966.
- Hargreaves, J. K.: Auroral Absorption of HF Radio Waves in the Ionosphere: A Review of Results from the First Decade of Riometry, *Proceedings of the IEEE*, 57, 1348–1373, 1969.
- Hargreaves, J. K.: *The Solar-Terrestrial Environment*, Cambridge University Press, 1995.
- Hargreaves, J. K. and Detrick, D. L.: Application of polar cap absorption events to the calibration of riometer systems, *Radio Sci.*, 37(3), 1035, doi:10.1029/2001RS002465, 2002.
- Hargreaves, J. K., Ranta, H., Ranta, A., Turunen, E., and Turunen, T.: Observations of the Polar Cap Absorption Event of February 1984 by the EISCAT Incoherent Scatter Radar, *Planet. Space Sci.*, 35, 947–958, 1987.
- Hargreaves, J. K., Shirochkov, A. V. and Farmer, A. D.: The polar cap absorption event of 19–21 March 1990: recombination coefficients, the twilight transition and the midday recovery. *J. Atmos. Terr. Phys.*, 55, 857–862, 1993.
- Juday, R. D. and Adams, G. W.: Riometer measurements, solar proton intensities and radiation dose rates, *Planet. Space Sci.*, 17, 1313–1319, 1969.
- Kavanagh, A. J.: Energy Deposition in the Lower Auroral Ionosphere Through Energetic Particle Precipitation, PhD thesis, Lancaster University, 2002.
- Kavanagh, A. J., Kosch, M., Honary, F., Senior, A., Marple, S. R., Woodfield, E. E., and McCrea, I. W.: The statistical dependence of auroral absorption on geomagnetic and solar wind parameters, *Ann. Geophys.*, 2004.
- Krucker, S. and Lin, R. P.: Two Classes of Solar Proton Events Derived from onset time analysis, *ApJ*, 542, 61–64, 2000.
- Leinbach, H.: Some Observations of daytime recoveries during polar cap absorption events, *Arkiv. Geofysik*, 3, 427–429, 1961.
- Leinbach, H.: Midday Recoveries of Polar Cap Absorption, *J. Geophys. Res.* 72, 5473–5483, 1967.
- Leske R. A., Mewaldt, R. A., Stone, E. C., and von Rosenvinge, T. T.: Observations of geomagnetic cutoff vari-

- ations during solar energetic particle events and implications for the radiation environment at the space station, *J. Geophys. Res.*, 30 011–30 022, 2001.
- Little, C.G. and Leinbach, H.: The riometer: a device for the continuous measurements of ionospheric absorption, *Proc. IRE*, 37, 315–320, 1959.
- Nielsen, E. and Honary, F.: Observations of Ionospheric Flows and Particle Precipitation Following a Sudden Commencement, *Ann. Geophys.*, 18, 908–917, 2000.
- Oguti, T.: Geomagnetic Bay Disturbance and Simultaneous Increase in Ionospheric Absorption of Cosmic Radio Noise in The Auroral Zone, *Rept. Ionosphere Space Res. Japan*, 17, 291–301, 1963.
- Patterson, J. D., Armstrong, T. P., Laird, C. M., Detrick, D. L., and Weatherwax, A. T.: Correlation of solar energetic protons and polar cap absorption, *J. Geophys. Res.*, 106, 149–163, 2001.
- Paulikas G. A., Blake, J. B., and Freden, S. C.: Low energy solar cosmic ray cut-offs: diurnal variations and pitch-angle distributions, *J. Geophys. Res.* 73, 87–95, 1968.
- Pierce, J. A.: VLF Phase shifts associated with the disturbance of February 23, *J. Geophys. Res.*, 61, 475–483, 1956.
- Potemra, T. A.: The empirical connection of riometer absorption to solar protons during PCA events, *Radio Sci.*, 7, 571–577, 1972.
- Ranta, H., Ranta, A., Yousef, S. M., Burns, J., and Stauning, P.: D-region observations of polar cap absorption events during the EISCAT operation in 1981–1989, *J. Atmos. Terr. Phys.*, 55, 1993.
- Rees, M. H.: *Physics and Chemistry of the Upper Atmosphere*, Cambridge University Press, 1989.
- Reid, G. C.: Current Problems in polar-cap absorption, in: *Inter-correlated Satellite Observations Related to Solar Events*, edited by Manno, V., and Page, D. E., 319–334, Reidel, 1970.
- Reid, G. C.: Polar-Cap Absorption – Observation and Theory, *Fundamentals of Cosmic Physics*, 1, 167–202, 1974.
- Reid, G. C. and Sauer, H. H.: The influence of the Geomagnetic Tail on Low-Energy Cosmic-Ray Cut-offs, *J. Geophys. Res.*, 72, 197–208, 1967.
- Rietveld, M. T. and P. N. Collis, Mesospheric observations with the EISCAT UHF radar during polar cap absorption events: 2. Spectral measurements. *Ann. Geophys.*, 11, 797–808, 1993.
- Shea, M. A. and Smart, D.F.: Solar proton event patterns: The rising portion of five solar cycles, *Adv. Space. Res.*, 29, 3325–3330, 2002.
- Schlegel, K. and St.-Maurice, J. P.: Anomalous heating of the polar E-region by unstable plasma waves 1. Observations, *J. Geophys. Res.*, 86, 1447–1452, 1981.
- Schunk, R. W. and Nagy, A. F.: Electron Temperatures in F-region of ionosphere-Theory and Observations, *Rev. Geophys.* 16, 355–399, 1978.
- Schunk, R. W. and Nagy, A. F.: Ionospheres of the terrestrial planets, *Rev. Geophys.*, 18, 813–852, 1980.
- Stauning, P.: Absorption of cosmic noise in the E-region during electron heating events. A new class of riometer absorption events, *Geophys. Res. Lett.*, 11 1184–11 1187, 1984.
- Van Allen, J. A., Lin, W. C. and Leinbach, H.: On the relationship between absolute cosmic ray intensity and riometer absorption, *J. Geophys. Res.*, 69, 4481–4491, 1964.